Received: 20 June 2023 | Revised: 20 September 2023 | Accepted: 24 September 2023

DOI: 10.1111/fog.12657

ORIGINAL ARTICLE

FISHERIES OCEANOGRAPHY WILEY

Concentration and condition of American lobster postlarvae in small-scale convergences

Jesús Pineda | Carolyn Tepolt | Vicke Starczak | Phil Alatalo | Sara Shapiro

Biology Department, Woods Hole Oceanographic Institution, Woods Hole, Massachusetts, USA

Correspondence
Jesús Pineda, Biology Department, Woods Hole Oceanographic Institution, Woods Hole, MA 02543, USA.
Email: jpineda@whoi.edu

Funding information
NOAA's American Lobster Initiative, Grant/Award Number: NA20OAR4170502

Abstract

Invertebrate larvae are often abundant in the surface ocean, which plays a key role in their dispersal and connectivity. Pelagic microhabitats characterized by small-scale hydrographic variability are complex and ubiquitous in the coastal ocean, but their study is challenging, and they have been largely neglected in meroplankton ecology. Surface convergences, i.e., surface microhabitats featuring convergent horizontal currents, may aggregate the last larval stage of the American lobster and could provide shelter and food for Stage IV postlarvae and thus enhance their condition. We tested these hypotheses by conducting a series of cruises in the southwestern Gulf of Maine in summer 2021, sampling 15 paired sets of potential convergences and off-convergence unstructured habitat. We measured postlarval abundance, surface hydrography, acoustic backscatter, and circulation. Experiments and image analysis compared condition, color, and morphology of postlarvae sampled inside and outside potential convergences. Potential convergences varied in near-surface hydrographic patterns, with most displaying consistency among two transects and diverse patterns in salinity and temperature (e.g., across-convergence gradients with equal or different signs). While the highest postlarval abundances were found in convergences, abundance patterns on and off convergences were not consistent, and another analysis indicated higher abundance in convergences than in a 7-year untargeted surface ocean data set. Experiments indicated no survivorship differences among convergence and non-convergence individuals at two temperatures, while image analyses revealed differences in color and size. Physical measurements and qualitative neuston community analyses indicated substantial heterogeneity among potential convergences. Our results reinforce that small-scale heterogeneities are highly variable but important to the ecology of meroplankton, including the pelagic and neustonic habitats where lobster postlarvae are abundant.

KEYWORDS
condition, convergences, *Homarus americanus*, postlarvae

1 | INTRODUCTION

Most marine benthic invertebrates have a complex life cycle where adults and larvae have distinct morphologies and occupy different habitats. In these species, adults have large fecundities, and mortality is high in the larval and juvenile stages, with potentially strong selection for the fittest individuals. Dispersal and connectivity among subpopulations typically occur during the larval phase, and larval and juvenile dispersal and recruitment are crucial to the population dynamics of these species (e.g., Hastings & Botsford, 2006). Knowledge of the different components influencing recruitment, a complex process dependent on early life history, behavior, and hydrodynamic processes, is necessary for a mechanistic understanding of population dynamics (e.g., Pineda et al., 2009). This synthetic understanding, in turn, is key to building accurate predictive frameworks to inform fisheries and conservation management.

Individuals that avoid mortality and enhance their condition during the larval phase increase their chances to disperse, recruit, and survive to reproduce. However, measuring predation rate, a large component of plankton mortality (e.g., Lima-Mendez et al., 2015; Smith & Herrkind, 1992; Verity & Smetacek, 1996), and characterizing diet and the processes associated with enhanced resource acquisition, remains daunting for most invertebrate larvae. The issues include the inherent difficulty of measuring mortality in a three-dimensional fluid environment (e.g., Ohman & Hirche, 2001; Rumrill, 1990) and a typically coarse characterization of bottom-up trophic processes and their temporal and spatial scales (e.g., the coarse temporal scales of the "spring bloom": Barnes, 1956; Platt et al., 2003). Small-scale heterogeneities in the coastal ocean such as fronts can offer a refuge from predation and be associated with elevated resource concentration, and meroplankton concentration can also be elevated in these features (e.g., Kingsford, 1993; Whitney et al., 2021). Although the importance of small-scale heterogeneities in the seemingly unstructured coastal pelagic habitat has long been recognized for marine metazoans (e.g., Hamner, 1988; Kingsford, 1993), these patterns and processes remain poorly described because of the difficulty in resolving small-scale features that can be unpredictable and ephemeral.

Small-scale pelagic habitat heterogeneities are associated with physical convergent and divergent processes, such as estuarine fronts, with surface across-front hydrographic gradients (Govoni & Grimes, 1992; O'Donnell et al., 1998) and internal waves (Alpers, 1985), with generally no surface hydrographic variability (but see Pineda et al., 2020, for highly nonlinear internal waves). Mixing can modulate the erosion of small-scale heterogeneities (O'Donnell, 1990), but upper layer mixing by strong winds (>10 m/s) and surface waves can also be associated with convergent and divergent Langmuir circulation (Kukulka et al., 2009). These features can be observed by the naked eye: for example, bands of rough and smooth water reveal internal waves, where rough waters are associated with convergences, while smooth waters (slicks) are associated with divergences (Alpers, 1985; da Silva et al., 1998). Convergent processes can be inferred from the accumulation of buoyant material such as flotsam and seagrass arranged linearly, and zooplankton can also accumulate in these microhabitats if they swim up against the downwelling currents associated with the convergence (e.g., DiBacco et al., 2011; Epifanio, 1987; Shanks, 1985; Zeldis & Jillet, 1982). Thus, accumulation of plankton in convergences can be passive, for flotsam and buoyant plankton such as gaseous cnidarians, and active, mediated by swim-up behavior, such as in some invertebrate larvae. While some studies have found that juveniles and larvae are concentrated in convergences (e.g., Zeldis & Jillet, 1982, for juvenile galatheid crabs and Pineda, 1999, for cyprid barnacle larvae) others have not (e.g., Clancy & Epifanio, 1989, for brachyuran crab larvae and Pineda, 1999, for bryozoan cyphonaute larvae).

H. americanus, the American lobster, has high fecundity, with individuals producing up to ~77,000 eggs (Campbell & Robinson, 1983), relatively few of which will survive to adulthood. The American lobster has a typical two-phase life cycle, encompassing a pelagic and a benthic phase. The pelagic phase includes three fully planktonic larval stages (Stages I–III) and a postlarval stage (Stage IV), which is largely planktonic until individuals eventually settle on bottom habitats and molt into juveniles (Ennis, 1995; Factor, 1995). Lobsters carry eggs for about a year before they hatch in the summer (approximately July–August); females with well-developed eggs sometimes aggregate in shallow waters, but hatching appears to occur over a broad range of habitats, from the shallow nearshore to deep offshore habitats (reviewed in Ennis, 1995). Larval duration (Stages I–III) is on the order of 22 days at the Magdalen Islands (Gendron et al., 2018), and settlement occurs from early August to early September in Maine (Wahle & Steneck, 1991). Larval duration is strongly dependent on temperature and other environmental factors (Ennis, 1995; Quinn, 2017). The I–III larval stages are more broadly distributed in the water column, but the postlarval pelagic stage IV tends to be found near surface waters (Harding et al., 1987), although postlarvae can sometimes be found in subsurface and deeper waters, depending on temperature. For example, in waters warmer than 12°C, postlarval depth distribution correlates with the 12°C isotherm (Annis, 2005). *H. americanus* larvae are omnivores, preying on zooplankton, particularly crab megalopae and copepods (e.g., Harding et al., 1982; Juinio & Cobb, 1992) and phytoplankton, and respond to increases in pressure (depth) by swimming up (Ennis, 1975). While larval supply is key for understanding lobster population dynamics (e.g., Fogarty & Idoine, 1986; Incze & Naimie, 2000; Incze & Wahle, 1991) and population connectivity (Fogarty, 1998; Incze et al., 2010), little is known about the small-scale pelagic habitat of larvae and postlarvae, its ecological heterogeneities, and the conditions that may be associated with successful foraging, growth, and survivorship in the species at this stage. A few studies have noted postlarvae in convergences (Cobb et al., 1983), including in Langmuir cells (Harding et al., 1982) and an association between high postlarval abundance and macroalgae (Grabe et al., 1983). Together with knowledge on postlarval behavior and distribution (Ennis, 1975), and other data on small-scale spatial heterogeneities, these observations suggest that convergences could be critical to the ecology and population dynamics of this species, influencing microhabitat environmental variability, larval transport, and foraging, with potential consequences for postlarval dispersal and survivorship.

In this study, we addressed the following questions: Are lobster postlarvae more abundant in convergences than outside them? Do postlarvae aggregate equally in all types of convergences? Are postlarvae in convergences in better condition than postlarvae outside of these features? What types of convergences occur in the Western Gulf of Maine? *H. americanus* postlarvae are excellent candidates to occur in surface convergences because they are neustonic and well equipped in terms of locomotion and behavior to exploit the fine-scale spatial heterogeneity of convergences. We hypothesized that postlarvae would be more abundant in convergences than outside convergences because convergent circulation may aggregate postlarvae and other resources and because these habitats may represent a rich foraging habitat and may offer postlarval lobsters a refuge from pelagic predators.

2 | METHODS

2.1 | Field measurements: Postlarval abundance and physical observations

Field work included nine cruises between 20 July and 12 August 2021, when *H. americanus* postlarvae have historically been abundant in southern coastal New Hampshire and Maine (Annis, 2004; Incze et al., 2000, 2006). Our sampling from the R/V Gulf Challenger (Univ. of New Hampshire) targeted coastal waters between Cape Ann, Massachusetts and Wells Bay, Maine (Figure 1) in sites ranging from 19 to 80 m in depth (33 m median; Table 1). The hypothesis was tested by sampling potential convergences, and in each case, a nearby area outside the potential convergence. To locate zones with active convergent circulation, we searched for linear features with concentrated surface material such as kelp, seagrass, and bubbles (Figure 2). The ease of detecting these features by eye varied from cruise to cruise, depending on sea conditions, which were generally calm. These

TABLE 1 Convergence ID, date, and tow length (in convergence) and outside convergence

ID	Date 2021	Depth (m)	Tow length (m)
C1	20-Jul	35	(952)/1,079
C2	21-Jul	37	(520)/408
C3	21-Jul	31	(937)/1,056
C4	22-Jul	21	(519)/458
C5	29-Jul	80	(1,062)/1,068
C6	3-Aug	33	(1,065)/1,046
C7	3-Aug	79	(539)/513
C8	4-Aug	38	(722)/726
C9	4-Aug	61	(872)/893
C10	4-Aug	33	(855)/842
C11	10-Aug	20	(896)/842
C13	10-Aug	19	(571)/666
C14	11-Aug	29	(771)/732
C15	11-Aug	30	(599)/773
C16	12-Aug	26	(766)/592

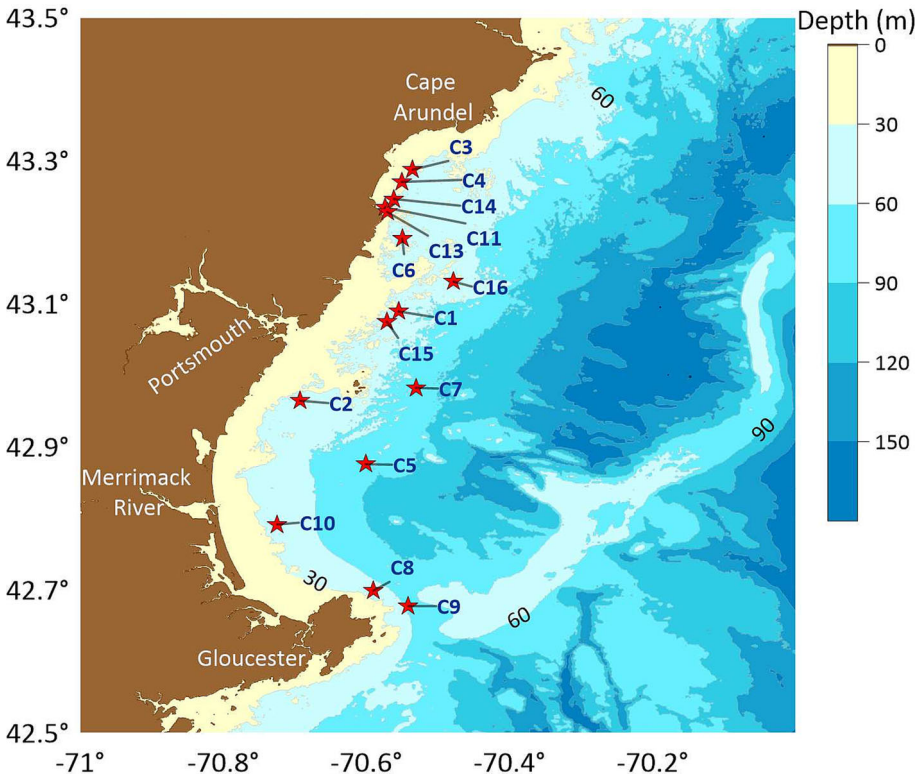

FIGURE 1 Potential convergences sampled in this study. The R/V challenger sailed from Portsmouth, New Hampshire. Digital bathymetry from the US Geological Survey (2013).

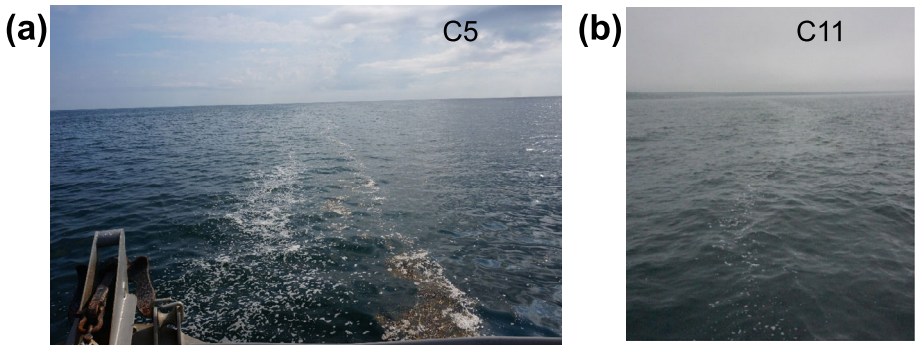

FIGURE 2 Convergences C5 (a) and C11 (b) (29 July and 10 August 2021). C5 is linear and visibly well organized, with bubbles and kelp well separated. C11 was also well organized, with low-contrast materials under the surface.

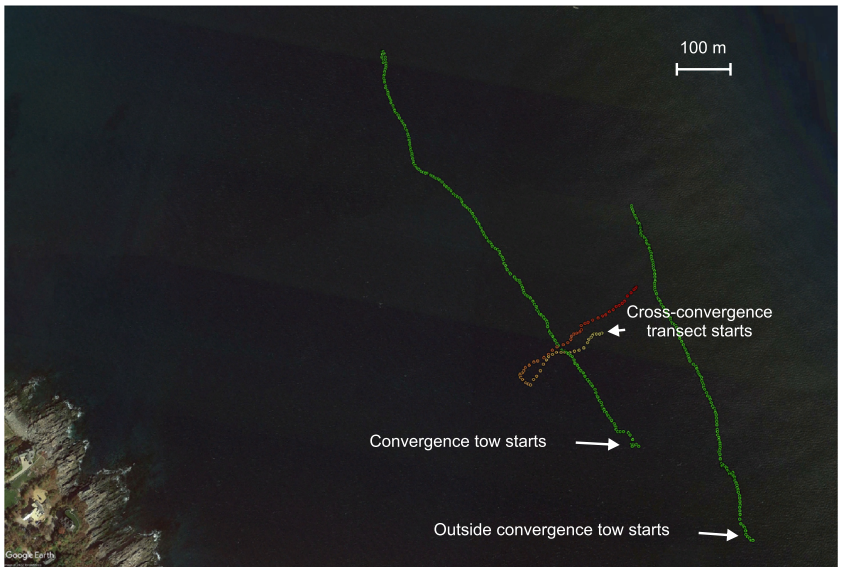

FIGURE 3 Transects across, along, and outside of convergence C11 from navigation data. Map image: Google Earth, Terrametrics.

features, however, are not necessarily associated with active convergent circulation, since the circulation concentrating surface materials may have lapsed while the surface materials themselves take time to disperse (i.e., "ghosts of active convergences"). Therefore, hereafter, we name features initially identified by eye as "potential convergences." Based on surface hydrographic patterns across the features examined a posteriori, and their consistency among the two crosses, potential convergences include "active convergences" and "inconsistent convergences." Features that were well organized in the short-axis (across) dimension, i.e., with kelp and foam on opposite sides (Figure 2a), were often associated with active convergences, as determined by subsequent physical measurements, and qualitative observations indicated that many potential convergences showed distinct zones of rough and/or smooth waters (e.g., Figure 2b), which are often associated with vertical currents (e.g., Alpers, 1985; Pineda, 1999). After a potential convergence was identified, sampling was initiated if the feature appeared linear and uninterrupted and had a minimum length of ~400–500 m (estimated by the R/V Challenger captain; Table 1). For each potential convergence, measurements included across-convergence surface hydrography, acoustic backscatter, and current profiling, followed by neuston sampling within and outside the feature (Figure 3). Particles such as plankton and physical microstructures (e.g., turbulence and bubbles) reflect sound, and acoustic backscatter can be used to determine the distribution of these features at fine spatial and temporal scales (e.g., centimeters and seconds) (e.g., Warren et al., 2003).

Potential convergences were crossed perpendicularly with two roughly parallel transects. Across-convergence measurements included surface hydrography (~1.5–2.5 m depth) by towing a Castaway CTD (Sontek), water column acoustic backscatter (Biosonics Extreme) with a 430 kHz transducer mounted in a pivoting boom on the boats' starboard side (~1m depth), and circulation using a 600 kHz RDI ADCP Workhorse (Teledyne) mounted in the vessel's hull (~2 m water depth). The ADCP measured east–west, north–south, and vertical currents, velocity reference was bottom tracking, and bin size was 1m, with a sampling frequency of one ensemble every 1.4 s (every ping). Data outliers were removed, a 5-point moving mean filter was applied, and currents were rotated in the direction perpendicular to the convergence (i.e., in the direction of the boat heading). Physical data across convergences were measured in the time reference and converted to distance using GPS position and boat ground speed. Potential convergences are described according to their across-patterns in surface salinity, temperature and density, and backscatter; ADCP data were used when available.

Biota were sampled using a neuston net (1.5 m width × 1 m height frame, 4 m net, and 1 mm mesh opening; Sea-Gear). Flotation

devices maintained the frame ~55 cm underwater, and a mechanical flowmeter (General Oceanics) estimated flow. The vessel sampled along the convergence in a pattern that crossed it from side to side in long swaths, sampling both sides of the convergence, including areas with and without visible accumulation of surface material. A second, paired tow was conducted alongside but outside of each potential convergence; for each pair of tows, tow duration was approximately the same. For each convergence, only one sample was taken inside the convergence and one outside it, and therefore, there was no within-feature replication. Boat ground speed along convergences was 1.2–1.9 knots ($\bar{x} = 1.6$ knots), tow time ~9–22 min ($\bar{x} = 16$ min), and tow length along potential convergences was 519–1,065 m ($\bar{x} =$ 776 m for potential convergences, and 780 m for areas outside convergences). Plankton sampling was terminated after sufficient distance was covered, or the net was full, or the boat reached the end of the feature. Sampled area was derived from flowmeter measurements and sampling length (from GPS). Abundance is reported as density to facilitate comparison with other American lobster larvae studies, which typically report No. m^{-2} (Annis, 2004; Harding et al., 1982; Incze et al., 2006).

2.2 | Plankton samples

Net samples were deposited in 25-l and 120-l plastic containers, depending on volume, and rinsed with coarse-filtered saltwater multiple times to separate the target samples from larger organisms including jellyfishes, and from flotsam including kelp, seagrass, wood, other terrestrial vegetation, and other natural and manmade items. Total flotsam volume was roughly measured to the nearest 1 L using marked buckets; smaller volumes were assigned to the closest volume of 0.5, 0.1 or 0 L. Small neuston (<2 cm on longest dimension) were collected from all rinse water using a 1 mm sieve. Live samples were scanned for *H. americanus* postlarvae, which were removed and photographed alive and individually in the field under natural sunlight conditions against a PortaBrace white balance card (B&H Photo Video, New York City, New York). All postlarvae identified at the time of sampling were photographed at least three times; a centimeter ruler and a WDKK Waterproof Color Chart (DGK Color Tools, Newton, Massachusetts) were included in each photograph as standard references. After photography, most lobster postlarvae were preserved in 95% ethanol. A subset of postlarvae was maintained alive in coolers and transported to Woods Hole, Massachusetts, within 8 h of collection for experimentation and additional photography (see details below). All other small neuston were preserved immediately in approximately 10–20 volumes of 95% ethanol; these included, but were not limited to, invertebrate and fish larvae, isopods, amphipods, copepods, juvenile mollusks, and terrestrial insects. Preserved samples from consistent convergences were sorted to identify and count any lobster postlarvae that were missed at the time of sampling; data on broader neuston composition within and outside convergences are being collected for a separate manuscript.

2.2.1 | Comparison with a seven-year data set

Our data, which specifically sampled within convergences, were compared with abundance data derived from long-term sampling of *H. americanus* postlarvae in the surface ocean (not targeted at convergences) in the same region and during the same time of the year. This comparison was used to evaluate whether postlarvae were more abundant in convergences than in the untargeted multiyear data set and whether abundance in our outside convergence tows was not different than in the larger data set.

Incze et al. (2006) present postlarval abundance data from neuston plankton tows from 1989 to 2003 by day of year (DOY) from 160 to 280, and by region along the Maine and New Hampshire coasts, including the region encompassing our sampling sites (Incze et al. fig. 5 bottom panel). Individual plankton tows targeting postlarvae in these sites include Maine lobster management zones (LMZ) F and G (southern Maine) and those in Seabrook New Hampshire (total $n_l = 924$ plankton tows, with postlarval abundance $\overline{x_l} = 1.47 \pm 5.51$). Most of these data originate from Seabrook, where three stations 2 km away from the shore were sampled weekly as a part of an ongoing monitoring program (see also Annis, 2004; Incze et al., 2000). Only data from DOY 201 to 224 were used, corresponding to the period sampled in this study in 2021.

The bottom panel of fig. 5 in Incze et al. was digitized using an automated routine in Origin 2022b (OriginLab Corporation), yielding $n_d = 722$ postlarval abundance data points, with a matching DOY. Digitized DOY was rounded to the nearest integer, and after correcting for small negative abundances due to artifacts from the digitizing procedure, postlarval abundance was $\bar{x}_d = 2.75$. We assumed that the higher mean in the digitized dataset than in Incze et al. fig. 5 was due to overlapping zero and low values that were not resolved by the digitizing routine (low and zero postlarval abundance values from tow data can be common, e.g., Incze et al., 2006). Thus, the digitized series was complemented with 202 low abundance values to approximate the statistics reported by Incze et al., yielding a new series *dc* with $n_{dc} = 924$ and $\bar{x}_{dc} = 1.49 \pm 5.48$. The 202 low abundance values were then haphazardly assigned to DOY 160–280. The "complemented digitized dataset" *dc* was subsampled between DOY 201 to 224, matching the period sampled in 2021, yielding a series *dcw* ($\bar{x}_{dcw} = 2.10 \pm 4.27, n_{dw} = 317$, for DOY 201–224). These data, *dcw*, were used for randomization analyses, discussed in Section 3.

2.3 | Laboratory experiments

2.3.1 | Sampling and condition experiments

Live postlarvae from a set of tows taken off Perkins Cove, Ogunquit, Maine, on the morning of August 10, 2021, were transported in refrigerated coolers to Woods Hole, Massachusetts, to conduct laboratory experiments on postlarval condition. These postlarvae came from active convergence C11 ($n = 34$) and three off-convergence tows taken just afterwards ($n = 19$). This focal region was chosen as it was

one of the few potential convergences to yield enough postlarvae for experimentation; four paired off-convergence tows were conducted instead of the standard one to collect a larger number of postlarvae for experiments. Postlarvae were transported and held live overnight in the laboratory in individual wells of an 18-well polystyrene parts box (The Container Store, Coppell, Texas) at 18°C. The following day, all postlarvae were photographed individually in the laboratory under identical conditions, including a standard 0.01 mm measure and color references.

After photography, postlarvae were placed in individual 1 L glass jars filled with 800 ml 1 μm filtered seawater. Jars were loosely capped and assigned to either an 18°C or a 25°C temperature treatment, with "within convergence" ($n = 24$) and "outside convergence" ($n = 14$) postlarvae split evenly between the two temperatures: 18°C represents a warm non-stressful temperature, while 25°C is stressful but not lethal (Quinn, 2017). Animals were maintained at these temperatures for the duration of the experiment in Percival incubators (Percival Scientific, Perry, Iowa) and were checked daily for mortality and molting. Two HOBO temperature loggers (Onset, Bourne, Massachusetts) were placed in jars of water in each incubator to temperature independently every 15 min; temperatures were stable except for June 4–5, when a power outage resulted in both incubators going to ambient temperature (approximately 22.5°C) briefly. For the duration of the experiment, water was completely exchanged with filtered seawater pre-equilibrated to experimental temperature three times per week; for the first 3 weeks, animals were individually photographed in the laboratory before each water change. Animals were not fed, although those which molted consumed their molts, and the experiment ended upon mortality of all animals. Days until molting and days until mortality were calculated for each individual; in most cases, animals molted from Stage IV postlarvae (beginning of experiment) to Stage V juveniles before the end of this experiment.

2.3.2 | Postlarval color and size

Color and size measurements were collected from postlarval field photographs from all consistent convergences ($n = 121$: 84 convergence postlarvae and 37 outside postlarvae), as well as from photos taken in the laboratory before and during survival trials. Laboratory measurements represented a subset of C11 postlarvae ($n = 38$: 24 convergence and 14 outside) also photographed in the field and were compared with field measurements to confirm the utility of photographs taken under field conditions. In addition, color was taken from laboratory photos on the 3rd ($n = 38$) and 5th day ($n = 22$) in the laboratory to explore color change over time.

Color measurements were taken from five regions of each postlarva: the chela, central cephalothorax, posterior cephalothorax, second abdominal segment, and fifth abdominal segment. Using Adobe Photoshop Elements 15, each of these regions was circled and blurred using a blurring tool to obtain an average color value for each region. The edited images were then opened in ImageJ v.1.53 t (Schneider et al., 2012), and HEX values were recorded for each of the five regions. The red, green, and blue values were extracted from each HEX value using the "HEX2DEC" function in Microsoft Excel v.2301 and depicted in RGB colorspace using the R package "ternary" (Smith, 2017). In addition, the red value of each of the five measured regions was individually compared between convergence and non-convergence zone postlarvae using Wilcoxon tests. To visually represent color differences, the combined RGB values for each region were plotted into color grids using R package ggpubr v0.4.0 (Kassambara, 2023).

Postlarval length was measured for both the field and in-lab photos using ImageJ; length was defined as the distance between the bottom of the eye socket to the end of the cephalothorax. For the field photos, length was measured up to four times for each individual PL in C11 using different photographs to estimate repeatability of measurement using at-sea photography. Symmetry measurements were also obtained from the in-lab photos (only available for C11) following the approach of Harrington et al. (2019). Briefly, two lines were added to each lobster image in Powerpoint (Microsoft): one that bisected the midline of the postlarva and another spanning the

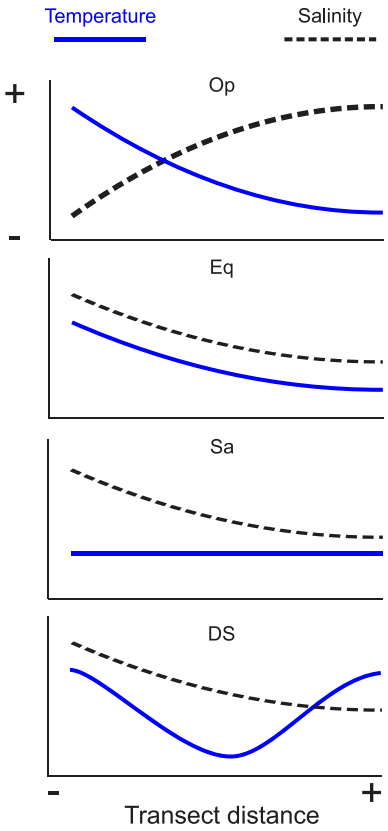

FIGURE 4 Schematic representation of cross-convergence surface salinity and temperature variability in active convergences. From top to bottom: opposite (Op) or equal sign (Eq), variability in salinity and temperature, only salinity (Sa) or temperature (not shown), and with different spatial scale of variability (DS). Hydrographic fronts are narrow zones with enhanced temperature and/or salinity gradients (e.g., Le Fèvre, 1986), and thus, the frontal zones would encompass the entire *x* axis.

cephalothorax laterally from the middle point of each eye. These edited images were then opened in ImageJ, and the measuring tool was used to quantify the distance between the midpoint of each eye socket to the midline of the cephalothorax, following the symmetry lines. The absolute value of the difference between left- and right-side measurements was the asymmetry value.

3 | RESULTS

3.1 | Hydrographic, backscatter, and circulation patterns across convergences

In total, we sampled 15 potential convergences. These were later classified as either active or inconsistent convergences based on the consistency of the surface hydrographic patterns among the two crosses. All 11 *active* convergences featured surface density gradients. In four *inconsistent* convergences, the patterns among the two crosses differed, and there was no other evidence of consistent convergent circulation (e.g., no evidence of physical convergence from currents). Thus, we limit most of our analyses to active convergences. Active convergences showed a diversity of hydrographic patterns, including salinity and temperature co-variability with opposite ($n = 3$; Op) or equal signs ($n = 3$; Eq), variability in only salinity ($n = 1$; Sa) or temperature ($n = 2$; Te), or with different spatial scales of variability for salinity and temperature ($n = 2$; DS) (Figure 4; Table 2). For example, in C5, salinity and temperature varied with opposite signs, while in C11, salinity and temperature varied at different spatial scales; C5 and C11 had consistent hydrographic patterns, while in C1, they were inconsistent (Figure 5; Table 2). For C5, the largest gradients in salinity and temperature were ~0.5 ps and 0.25°C, and for C11, they were ~0.5 ps and 0.15°C (Figure 5; Table 2); both C5 and C11 had regions of relatively low salinity.

Hydrographic gradients coincided with surface backscatter in eight convergences, though three active features displayed no backscatter patterns. Backscatter patterns, which may indicate plankton, bubbles, or other sound-reflecting features, extended from 3 to 8 m ($\bar{x} = 4.6$ m; Table 2), with the deepest consistent with an internal wave of depression (C7).

Currents and backscatter are presented for two active convergences. C5 was oriented northeast and featured strongly sheared across-convergence flows, with northwest currents in the upper 10 m (positive 332°T), and the fastest currents centered at 9 m, reversing to southeast below 12 m, with weaker deeper currents (Figure 6a). Thus, the upper water column from the surface to ~16 m was strongly sheared. Surface northwest (positive) currents were about the same in the first and second portions of the transects (i.e., from the start of the transect to ~<130 m and from ~130 to the end). The backscatter zone was restricted to shallow waters (~3 m) and coincided with the largest gradients in temperature and salinity (~ 76–130 m; Figure 5d). Thus, while accumulation of material and hydrographic patterns in C5 suggests convergence, there is no evidence of convergent circulation from the ADCP transect.

Across-convergence currents in C11 (positive 51°T) were directed roughly southwest, with weaker currents in deeper waters. Southwest currents were relatively slow from the surface to ~10 m in the first 70–80 m, with faster currents after 80 m: mean southwest currents in the top 10 m were ~35% slower in the first 80 m than

TABLE 2 Hydrographic patterns in convergences from surface measurements.

ID	Salinity (S) and temperature (T) surface gradients	Inconsistent (I); variability in only salinity (Sa) or temperature (Te); co-variability in salinity and temperature with opposite (Op) or equal (Eq) sign, and with different spatial scales for salinity and temperature (DS)	Backscatter patterns and maximum amplitude (m)
C1	ST	I	–
C2	T (1°C)	Te	3.5 m
C3	T (0.8°C)	Te	3 m
C4	ST (0.1 ps, 0.2°C)	Op	5.5 m
C5	ST (0.5 ps, 0.3°C)	Op	3 m
C6	ST (0.3 ps, 0.3°C)	Eq	No
C7	ST (0.15 ps, 0.5°C)	Eq	8 m
C8	S	I	–
C9	ST (0.5 ps, 1.8°C)	Op	No
C10	S (4 ps)	Sa	6.5 m
C11	ST (0.5 ps, 0.15°C)	DS	6.5 m
C13	ST (0.5 ps, 0.15°C)	DS	No
C14	ST (0.15 ps, 0.6°C)	Eq	3 m
C15	T	I	–
C16	T	I	–

Note: All consistent convergences but C7 had surface density patterns, and C7 backscatter occurred over an internal wave of depression.

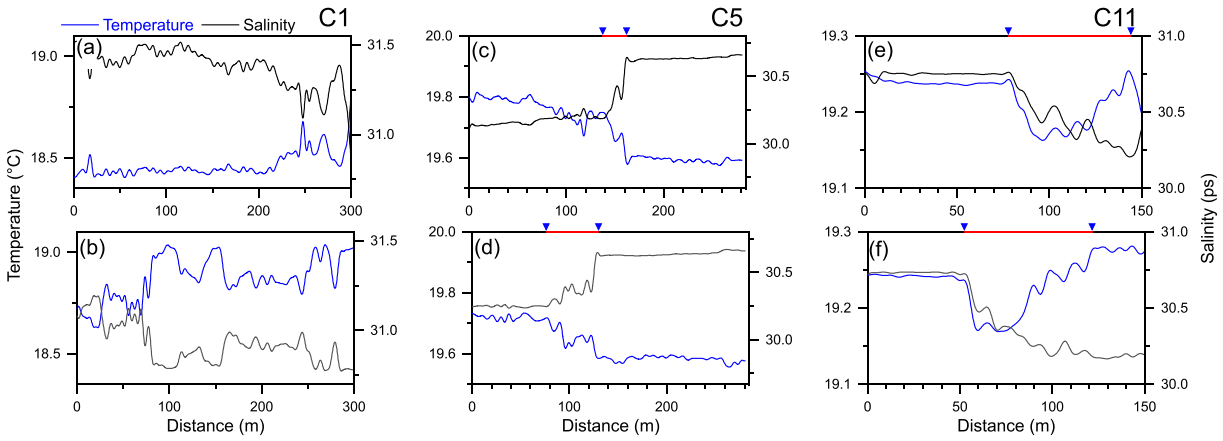

FIGURE 5 Temperature and salinity surface patterns for active (C5 and C11) and inconsistent convergences (C1). The upper panels (a, c, and e) display the first transect across the potential convergence, while the lower panels show the second pass (b, d, and f). Horizontal red lines on top of C5 and C11 panels mark the zone with the largest hydrographic gradients (i.e., the frontal region). Pictured convergences show co-variability in salinity and temperature with opposite sign (C5), different spatial scales for salinity and temperature (C11), and inconsistent hydrography patterns (C1).

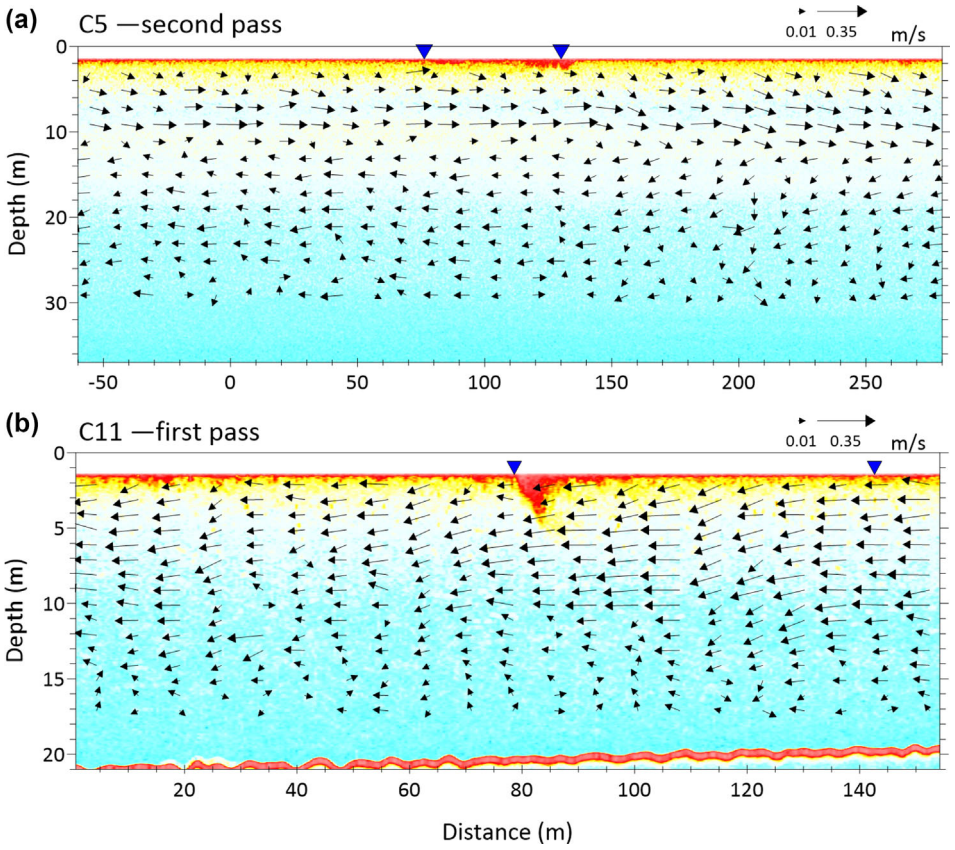

FIGURE 6 Circulation and backscatter in active convergences C5 second pass (a) and C11 first pass (b). Positive currents in C5 are 332°T and 51°T in C11. Bottom depth was 80 m in C5 and 20 m in C11. The sections with the largest hydrographic gradients (Figure 5) are bracketed by two blue triangle symbols near the surface. (The red feature along the transect at ~20 m in C11 b is the bottom).

after 80 m (0.11 vs. 0.16 m/s). The region with the largest hydrographic gradients corresponded to a zone of strong backscatter to 5–6 m at ~90 m, with weak downwelling (70–90 m), and a sharp gradient in temperature and salinity (Figure 5e). Thus, accumulation of material, circulation, hydrography, and backscatter all suggest physical convergence in C11.

3.2 | Postlarval abundance: Hydrographic patterns and regional variability

Postlarval abundance in net tows ranged from 0 to 34 in active convergences and 0 to 8 outside active convergences (0 to 10 in potential convergences). Mean postlarval density (No./1,000 m^2) was higher in

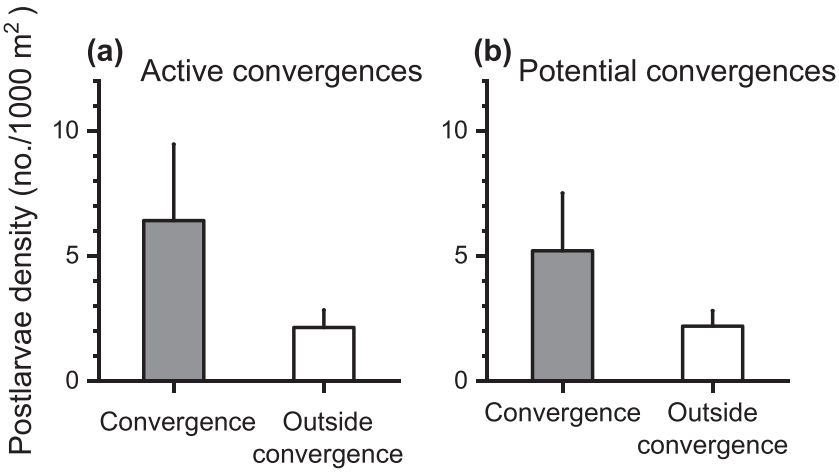

FIGURE 7 Postlarval density in active and all potential convergences (active and inconsistent) and outside. $n = 11$ for active features (a), and $n = 15$ for potential convergences (b).

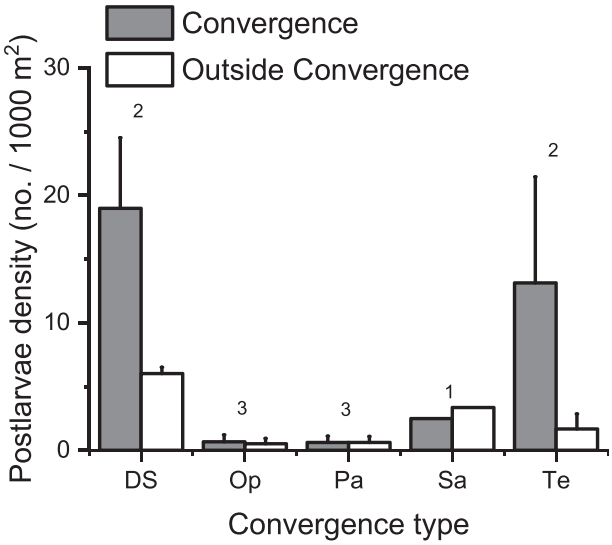

FIGURE 8 Postlarval density by active convergence hydrographic type and corresponding densities outside active convergences. Labels are sample size, which is the same for convergences and outside convergences. Surface temperature and salinity variability: at different spatial scales (DS), with opposite sign (Op), same sign (Pa), only in salinity (Sa), or only in temperature (Te).

active convergences than outside them ($\bar{x} = 6.41$ vs. 2.14) and higher in *all potential convergences* than outside them ($\bar{x} = 5.21$ vs. 2.19) (Figure 7), with the highest postlarval density in active convergences C3, C11, and C13 ($\bar{x} = 20.95$). Multiple additional tows outside C11 targeting animals to be used in experiments yielded relatively few postlarvae, confirming the extraordinarily high densities in C11. Postlarval abundance was highest in convergences where temperature and salinity varied at dissimilar scales (DS, Table 2), followed by patterns with only temperature variability (Te), with the lowest abundance in features with only salinity (Sa), and opposite and parallel (Op and Pa) gradients in temperature and salinity (Figure 8). The occurrence of relatively cool surface water in C11 (e.g., 60 to 110 m in Figure 5f), the circulation indicating physical convergence (Figure 6), and the high backscatter in a columnar pattern consistent with vertical circulation suggests that C11 featured active convergent circulation.

Postlarval abundance was generally higher at and north of Bald Head Point than in more southern sites, both in terms of samples from outside convergences, and samples from all potential convergences (Figure 9). We found more flotsam in convergences than outside them (convergence: 23.4 ± 9.9 L, outside: 0.1 ± 0.03 L, $p = 0.006$ with paired Wilcoxon test), though flotsam volume inside convergences varied widely and was not correlated with postlarval abundance ($p = 0.7$, linear regression).

3.3 | Postlarval abundance patterns: Randomization analyses

3.3.1 | Sampled postlarvae

The statistical hypothesis that mean abundance of postlarvae in convergences was larger than outside convergence zones was tested with a randomization analysis. This analysis included only convergences with consistent hydrographic patterns ($n = 11$). First, a paired t test among the two groups was conducted (one-tailed test), yielding a t statistic ***to***. Then, $i = 10{,}000$ paired two-sample t tests (1-tail) were computed, where each observed data point was randomly assigned to one of the two groups, yielding 10,000 t statistics ***tr***. Significance was calculated as $p = [1 - (\#\ \mathbf{tr} > \mathbf{to})/10{,}000]$ (Manly, 1997), yielding $p = 0.0671$ (Figure 10).

3.3.2 | Seven-year data set vs. sampled postlarvae abundance

Using the data derived from digitizing the bottom panel of fig. 5 from Incze et al. (2006), the following statistical hypotheses were tested

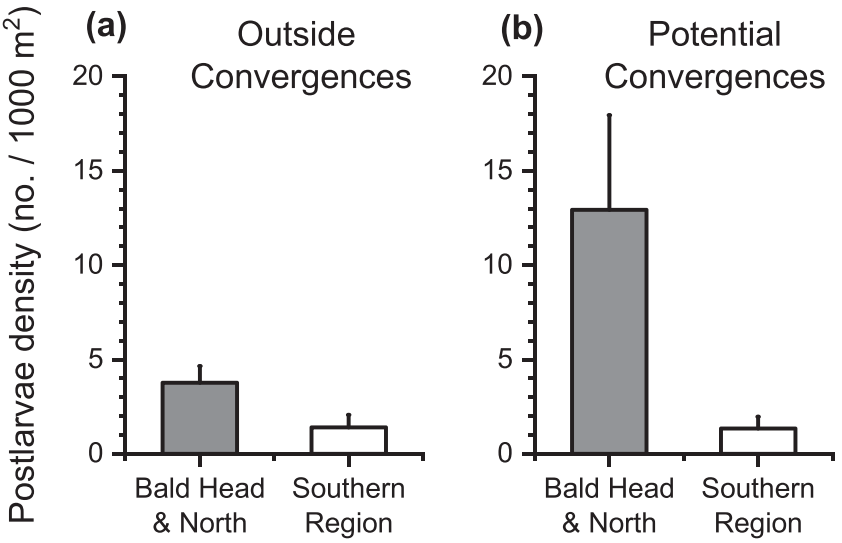

FIGURE 9 Postlarval abundance by region outside convergences (a) and in potential convergences (b) ($n = 15$). Bald Head and north included C3, C4, C11, C13, and C14, and the southern region included the remaining sites.

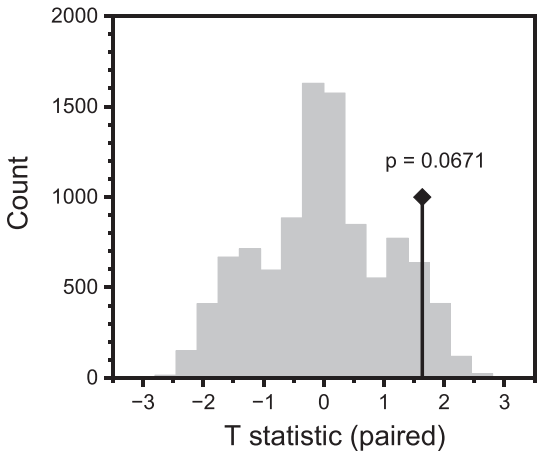

FIGURE 10 *t*-statistic frequency distribution of randomized paired consistent convergences vs. outside convergences areas ***tr***, with the computed *p* value.

using randomization analyses: (a) Mean abundance of postlarvae in consistent convergences ($n = 11$) is larger than untargeted surface ocean postlarval abundances from the 7-year data set ($n = 317$), and (b) mean abundance outside all potential convergences ($n = 15$) is different from digitized postlarval abundances ($n = 317$).

The randomization procedures were broadly similar to the one described above, with the following exceptions. The *t* test for (a) included postlarval abundance in consistent convergences ($n = 11$) and the 7-year data set ($n = 317$), yielding ***to*** (pooled variances, one tail test), and the 10,000 *t* tests were calculated using randomly assigned data from the two groups to generate 10,000 *t* statistics ***td*** (pooled variance, one tail), with significance calculated as $p = [1 - (\#\ \mathbf{td} > \mathbf{to})/10{,}000]$, yielding $p = 0.0121$. The same procedure was followed for (b), testing differences between postlarval abundance outside convergences and the 7-year data set, but applying a two-tailed test, resulting in $p = 0.4038$ (Figure 11).

3.4 | Postlarval color and size

The greatest color variation was observed at two of the five tested postlarval regions: the posterior cephalothorax and the second abdominal segment; these regions had similar color values to each other, and we focus our subsequent analyses on the second abdominal segment. While color differences between convergence and non-convergence zone postlarvae were not consistent across all postlarvae, in C11, the postlarvae from outside convergence zones were redder than those inside convergence zones (Figure 12). This color difference was significant both for the full set of field-photographed postlarvae and for the subset subsequently photographed in the laboratory under controlled lighting conditions (field: $p = 0.01$; lab: $p = 0.002$) and was increasingly muted after 3 and 5 days under standard laboratory conditions (3 days: $p = 0.03$; 5 days: $p = 0.05$). (After 5 days, the majority of postlarvae had molted to early juveniles, which was associated with a strong red color shift, and were no longer comparable to postlarvae.) Color did not significantly differ in C3, C10, or C13 ($p > 0.05$ in all cases), the only other convergences with ≥3 postlarvae in each category.

Over all samples based on field photo single measurements, postlarvae captured in convergences were slightly but significantly smaller than those captured outside of them (length inside = 4.59 ± 0.51 mm; length outside = 4.89 ± 0.83 mm; $p = 0.0002$); mean standard deviation across three to four field photos of the same individual was 0.158 mm. This was driven in large part by postlarvae in C3 (length inside = 4.54 ± 0.84 mm; length outside = 5.10 ± 2.56 mm; $p = 0.009$) and C11 (length inside = 4.57 ± 0.78 mm; length outside = 4.93 ± 1.12 mm; $p = 0.002$); postlarvae in C10 and C13 did not show size differences ($p > 0.05$). Additional measurements from lab photos for C11 found a similar but not significant pattern of larger postlarvae outside convergences (lab photos: length inside = 4.80 ± 0.98 mm; outside length = 5.10 ± 1.36 mm; $p = 0.2$). There was no evidence for symmetry differences inside and outside

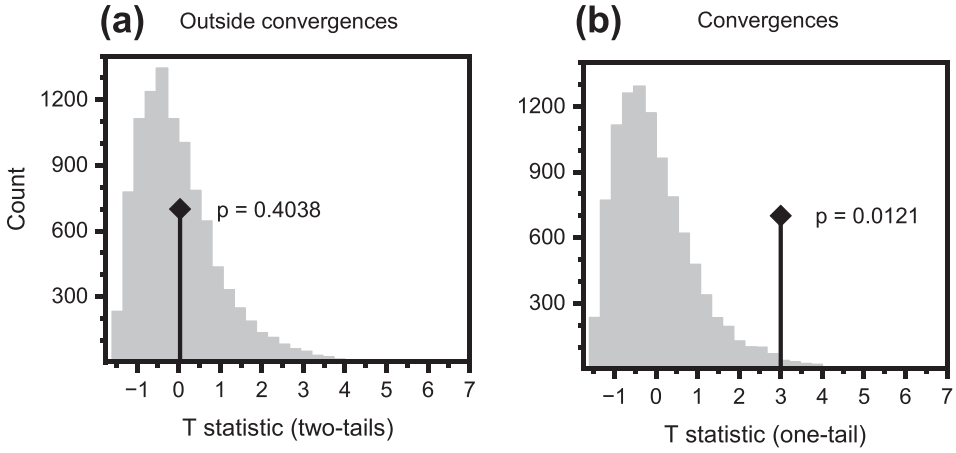

FIGURE 11 *t*-statistic histogram of randomized abundances in consistent outside convergences zones ($n = 11$, panel a) and consistent convergences ($n = 11$, panel b) vs. Incze et al. (2006) digitized data ($n = 317$), with p values.

convergence C11, the only feature for which high-quality lab photos were available (inside asymmetry: 0.14 ± 0.02 mm; outside asymmetry: 0.14 ± 0.02 mm; $p = 0.8$).

3.5 | Postlarval condition

Survival did not differ significantly by origin inside or outside convergence C11 within a temperature treatment (18°C: $p = 0.5$; 25°C: $p = 0.2$; Figure 13). Similarly, there was no difference of origin on time until postlarval molting to the first juvenile stage (Stage V) within a temperature (18°C: $p = 0.7$; 25°C: $p = 0.6$). Given this, animals were pooled within a temperature treatment regardless of their origin within or outside convergence C11 to explore molting and survival differences with temperature.

Nearly all Stage IV postlarvae molted to Stage V juveniles soon after arriving in the laboratory, after 5.2 ± 0.5 days at 25°C or 8.4 ± 0.5 days at 18°C ($N = 19$ for each temperature); molting occurred significantly faster at the elevated temperature ($p < 0.0001$). In total, animals survived for 40 ± 1.1 days at 18°C, significantly longer than the 23.8 ± 1.0 days they survived at 25°C ($p < 0.0001$). Three postlarvae held at 25°C failed to molt in the laboratory (two from within and one from outside the convergence); these postlarvae appeared to die slightly earlier than animals which molted to Stage V (18 ± 3.6 days survival vs. 24.9 ± 0.7 days for animals which molted), but this difference was not significant ($p = 0.1$).

4 | DISCUSSION

This research supports the idea that small-scale pelagic heterogeneities are important in *H. americanus* organismal and population processes. Work highlighting the importance of such features in juvenile fitness and population dynamics has emphasized fish (Castro et al., 2002; Kingsford, 1993), while other work has found that such features can be associated with larval transport enhancing recruitment (reviewed in Pineda & Reyns, 2018). Small-scale pelagic heterogeneities featuring convergent currents are difficult to track and measure, have short temporal scales, can be unpredictable in the short term, and have not been well studied. Little is known of the fundamental patterns and processes by which these features may impact *H. americanus* postlarvae, and this work is one of the first to address these phenomena.

4.1 | Abundance patterns: Regional processes and convergence types

Peak convergence postlarval densities in 2021 were very high compared to the maximum values in a 1989–2003 data set that did not specifically target convergences (Incze et al., 2006), while abundances outside convergences and in the digitized set were similar ($\bar{x} = 2.19$ in 2021 vs. 2.10 in 1989–2003), suggesting no substantial changes among the two periods. The large tow-to-tow abundance variability in 2021 is common in *H. americanus* postlarvae samples (e.g., Greenstein et al., 1983; Incze et al., 2006).

The highest postlarval densities in active convergences, with values up to ~3 standard deviations above the overall mean, were drawn from the northern sampling region (C3 and C11). Background abundance (i.e., outside convergences) was similarly higher in the northern region. Consistent patterns in postlarval abundance at tens of kilometer scales are common (e.g., Fogarty, 1983; Incze et al., 2006), and regional variability within the sampled region might ultimately determine abundances in convergences. These convergences, located at and north of Bald Head Point and off Israel Head and Ogunquit Beach in southern Maine, were sampled near the beginning and end of the sampling period and were close to each other, within 7 km. We hypothesize that higher abundance in C3 and C11 relate to the higher background densities in the local area (few km^2), with aggregation in the small-scale convergences (hundreds of meters) operating on these high abundances. In other words, with no postlarvae to be aggregated, biological and physical concentration mechanisms would not operate, as has been argued for larval transport (e.g., Pineda & Reyns, 2018). An alternative process, long distance postlarval accumulation and transport by small-scale propagating convergences from remote regions (few to tens of kilometers) is unlikely,

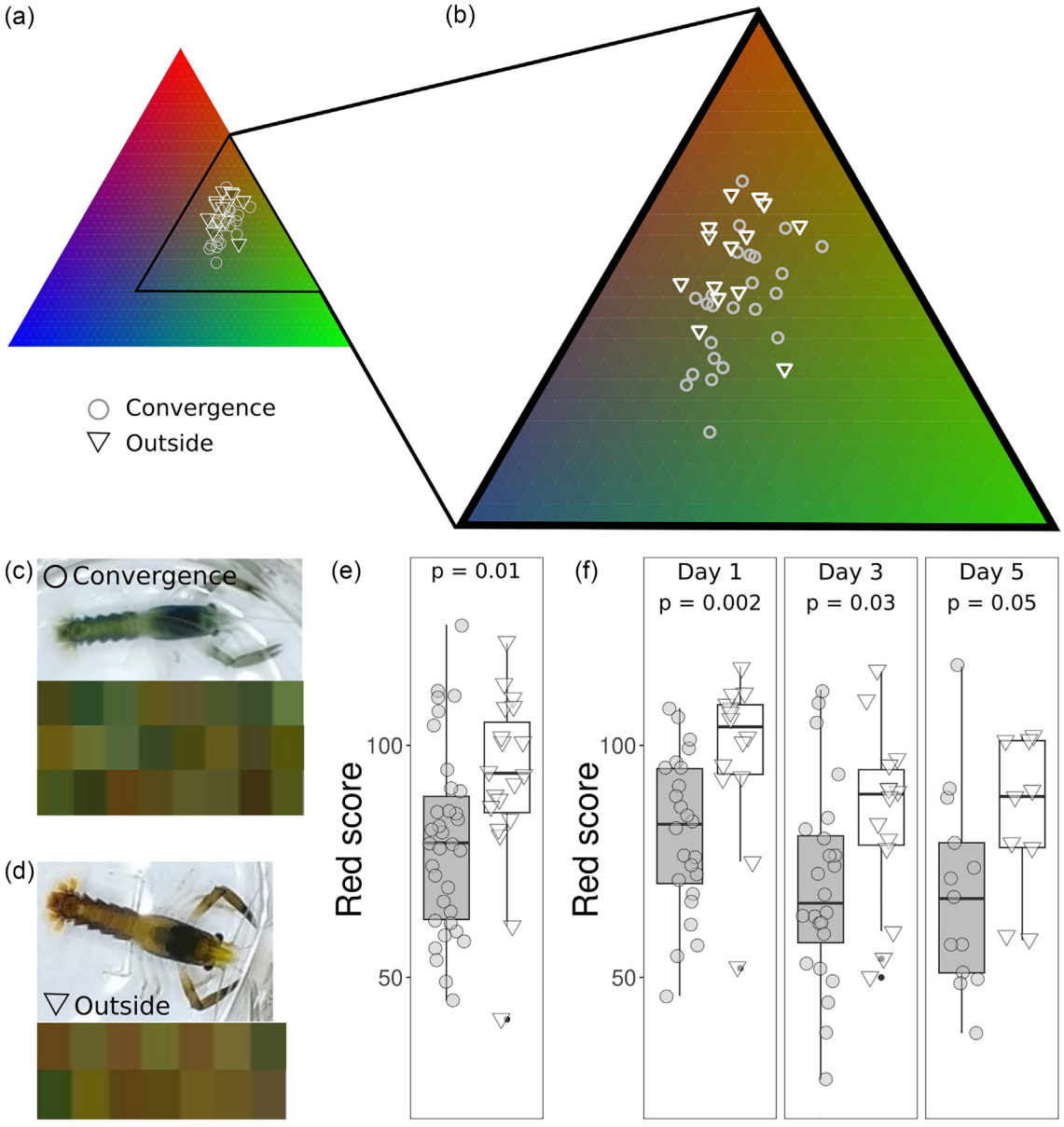

FIGURE 12 Color differences between postlarvae collected from inside and outside convergence C11. (a, b) Ternary plot of individual postlarval color from laboratory photos (a), with black inset highlighting the postlarval colorspace expanded in (b). (c, d) Laboratory photos of example postlarvae from inside and outside C11, with squares showing colors for each individual in each group. (e) Red value (from RGB color) of all postlarvae inside and outside C11, based on field photos. (f) Red value (from RGB color) of C11 postlarvae after 1, 3, and 5 days under consistent lighting conditions in the laboratory. Note that numbers are lower for Day 5, as 16 postlarvae molted to Stage V between 3 and 5 days in the lab, and were removed from this comparison.

as there is no evidence of such features. In addition to regional factors, hydrodynamics may also explain high postlarval abundances, as two of the highest abundance features (C11 and C13) had similar hydrographic patterns.

Studies that resolved convergences with hydrographic and current measurements found that features such as internal tidal bore warm fronts (Pineda, 1999) and upwelling fronts (Shanks et al., 2000) have high densities of certain meroplankton species, with a few exceptions: brachyuran crab larvae in tidal estuarine fronts (Clancy & Epifanio, 1989), and bryozoan larvae in an internal bore warm fronts (Pineda, 1999) were not concentrated. Surface hydrography and backscatter patterns indicated that C3, with temperature and backscatter gradients across the convergence, and C11 and C13, where temperature and salinity varied across the convergence at different spatial scales, had the largest postlarval densities. In particular, circulation and backscatter patterns in C11 are consistent with physical convergence. On the flip side, postlarval abundance was low for temperature and salinity co-variability with the same or opposite sign or with only salinity gradients. Some active convergences with these patterns were likely associated with river plume fronts, such as C5, near the

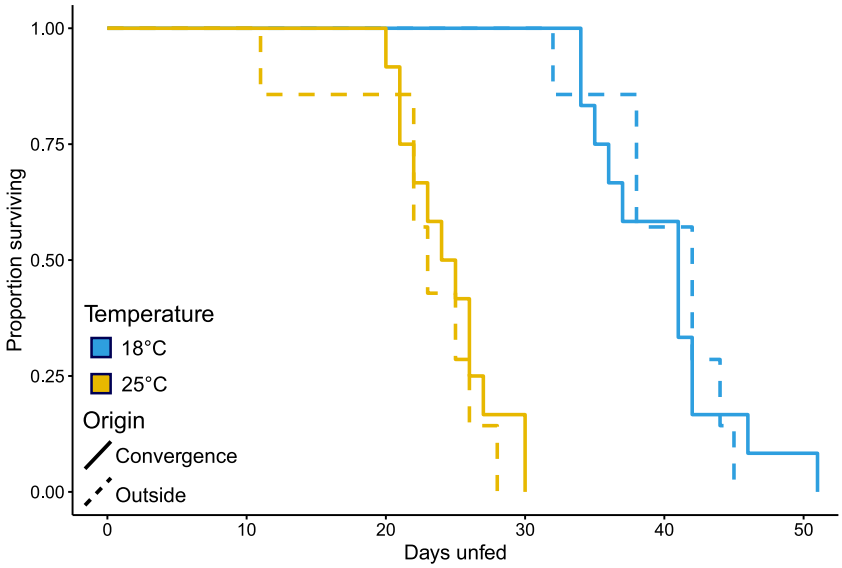

FIGURE 13 Kaplan–Meier functions displaying survivorship proportion of starved lobster postlarvae originating within and outside active convergences and at two different temperatures, 18°C and 25°C. Most postlarvae molted to Stage V juveniles during this experiment, and their full time to mortality (including in stage V) is shown here.

Merrimack River, while backscatter patterns in C7 (not shown) indicated convergence associated with internal waves of depression. The phase of the tide can influence the erosion of riverine plumes (O'Donnell, 1990), implying that the tide may modulate the aggregation of postlarvae in riverine plumes.

The convergences in this study tended to be hundreds of meters in length, and although their time scales were not formally measured, some were observed to be ephemeral and disintegrated during plankton sampling. Thus, postlarval residency in these features was transient, on the order of several hours. These convergences likely form, disintegrate, and reform with periodic processes such as the tide, tidally generated internal waves, and riverine fronts interacting with diurnal winds, implying that some postlarvae undergo repeated cycles of aggregation, as suggested by postlarval color that shifted over days (discussed below). The hydrodynamic mechanisms associated with most active convergences could not be resolved, as deriving across-convergence hydrographic profiles was not possible due to the ephemeral nature of these features and competing plankton sampling, and our sample size was relatively low. Future studies should resolve the nature of these convergences with more dedicated sampling, to enable more detailed hydrodynamic characterization of convergences where larvae accumulate.

Larval accumulation in small-scale ephemeral convergences results from an interaction between the horizontal flows and the plankton behavioral response or physical properties (buoyancy) in the face of downwelling flows (e.g., Le Fèvre, 1986). Invertebrate larvae might also accumulate in small-scale divergences if they would swim against upwelling circulation. Accumulation in divergences might be rare because, as opposed to convergences, the vertical flows associated with upwelling in the ocean occur over extended areas, and cues might be insignificant for the larvae. An exception might be Langmuir cells, where divergence tends to occur over small spatial scales (10–100 m's).

4.2 | The role of convergences and temperature in postlarval survival

Despite convergences representing potentially rich sources of prey, we observed no differences between convergences and outside areas in postlarval condition, as measured by unfed survival. While this should be regarded as a preliminary result since it was based on animals from a single convergence and sample size was small, this may be consistent with our understanding of convergences and larval biology. As with other marine invertebrates, larval mortality in lobsters is highest at the earliest stages of larval development, while postlarvae and newly settled juveniles are much more robust (Bartley et al., 1979; Rumrill, 1990), although this varies depending on predator preference (Pennington et al., 1986). Since convergences are often transient, a postlarva's presence in any given convergence is likely to represent a small fraction of its total time spent in that stage, although in cases where convergences reform due to periodic processes, total time spent may be longer. However, convergences may play an important role in the survival of more vulnerable early larval stages, which are shorter in duration and more sensitive to food availability and brood-to-brood differences in yolk reserves (Anger et al., 1985; Templeman, 1936). These potential increases in survivorship in convergences, which are known for juvenile fish (e.g., Castro et al., 2002; Kingsford, 1993), were not addressed in this study but would be a fruitful avenue of future research.

While overall unfed survival was high, we also observed significantly faster mortality at 25°C (23.8 days) than at 18°C (40 days). This is consistent with the critical role that temperature plays in larval and juvenile growth, stage duration, and survival across many taxa including lobsters (Ennis, 1995; Quinn, 2017). Prior work on individually labreared juvenile lobsters (starting at Stage IV) found that the time to 50% mortality of starved animals was 46–47 days at 20°C or 25°C, increasing to 79 days at 15°C (Bartley et al., 1979). (While this survival is considerably higher than we observed, those animals were held in

flow-through environmental water passed through "high-rate sand filters," and it is likely that they were still able to feed on small particles although they were deprived of the experimental *Artemia* diet.) The pelagic postlarval stage tends to be found near surface waters (Harding et al., 1987), although some postlarvae can be found in subsurface and deeper waters, depending on a range of factors including salinity, ontogeny, and temperature. For example, in waters warmer than 12°C, postlarvae depth distribution correlates with the 12°C isotherm (Annis, 2005). We found some suggestion that the postlarvae found in convergences were smaller than those outside them, but this requires additional sampling and finer measurements to test convincingly. If true, it might suggest that convergences offer particular benefits to smaller animals or that these individuals might not be able to swim away from these features.

4.2.1 | Color variation and postlarval microhabitat

Color in crustaceans is determined in part by chromatophores in the integument, and many species can change their color transiently without molting (Stevens, 2016; Umbers et al., 2014). This process of physiological color change is under neuroendocrine control, with a range of neuroregulatory compounds contributing to color-changing abilities (Fingerman, 1985). Marine crustaceans may change color for improved camouflage (Hultgren & Mittelstaedt, 2015), or in response to UV light exposure, as has been demonstrated for some larvae and krill (Auerswald et al., 2008; Gouveia et al., 2004). The time frame on which these changes can occur has not been well-studied, but appears to be on the order of minutes to days for crustaceans (Auerswald et al., 2008; Umbers et al., 2014). In Stage IV and V *H. americanus*, color shifts to more red within a few hours after eyestalk ablation; this color shift is associated with changes in sodium regulation and can be reversed if eyestalk tissue is re-implanted (Charmantier et al., 1984). Here, we found that all postlarvae became less red under constant laboratory conditions, although the difference between "inside" and "outside" convergence postlarvae remained significant through 3 days. Observed color differences across two convergences in our study are broadly consistent with the casual observation that the color of lobster postlarvae may be due to associations with seaweed flotsam that accumulates in convergence zones (Harding et al., 1982). Grabe et al. (1983) found that postlarvae and macroalgae abundance were related; by contrast, Cobb et al. (1983) reported individual postlarvae actively avoiding weed. While we found more flotsam in convergences than outside them, postlarval abundance was not correlated with flotsam volume inside convergences. Interestingly, postlarvae outside the C11 convergence appeared redder than those within it; this pattern was not observed for C3 and C13 (the only other convergences with sufficient sample sizes for independent comparisons) or over all convergences. While these data are preliminary, we suggest that postlarval coloration may change in the short- to mid-term based on microhabitat differences in cover and/or UV exposure, reflecting the nature and consistency of each individual postlarva's recent environment.

5 | CONCLUSIONS

Studies on American lobster larval supply processes typically focus on a coarse characterization of the habitat and trophic processes; however, individual larvae often exploit small-scale microhabitats and experience their environment at much finer spatio-temporal scales (e.g., Metaxas, 2001). Postlarvae were more abundant in small-scale convergences, and coloration differences were also detected; however, no differences in survivorship were identified between individuals in and outside convergences. The importance of convergences as a neustonic microhabitat for postlarvae of the American lobster is potentially fourfold: as a neglected ecological heterogeneity that may aggregate prey (e.g., crab larvae and insects), as a potential factor in larval dispersal, as a microhabitat with higher postlarval densities resulting in reduced predation and enhanced survivorship (e.g., Rumrill, 1990), and, finally, as a source of error in sampling assessments of postlarval abundance, as patchiness due to aggregation in convergences will result in biased estimates when convergences are ignored (discussed by Harding et al., 1982). The ubiquity and overall importance of these pelagic microhabitats in shaping larval lobster diet and fitness are unknown, and these features themselves are not well-characterized, obscuring our understanding of their role in lobster population dynamics. More research is needed to advance knowledge on trophic interactions, fitness, and the biological-physical processes that promote recruitment at a crucial stage in the population dynamics of the American lobster. Finally, the finding that a sizable portion of postlarvae inhabit convergences suggests that managers and researchers should reconsider the biological-physical models that are appropriate to simulate larval dispersal of *H. americanus* larvae, including modeling of population trajectories in the face of ocean warming.

AUTHOR CONTRIBUTIONS

Jesús Pineda and Carolyn Tepolt conceived the project, executed the research, analyzed the data, prepared the figures, and wrote the paper. Vicke Starczak and Phil Alatalo executed the fieldwork, Sara Shapiro conducted the image analysis, and all authors edited the manuscript.

ACKNOWLEDGMENTS

We would like to acknowledge the excellent support in the field from the crew of the R/V Gulf Challenger, Captain Bryan Soares, and John Long and help in the lab from Corey McElroy, and Shayla Flaherty. For additional assistance, we thank the crew of the R/V Tioga and Eric Annis. Finally, we appreciate and acknowledge funding from NOAA's American Lobster Initiative (NA20OAR4170502) and the Woods Hole Oceanographic Institution.

CONFLICT OF INTEREST STATEMENT

The authors declare no conflicts of interest.

DATA AVAILABILITY STATEMENT

The data that support the findings of this study are available from the corresponding author upon reasonable request.

ORCID

Jesús Pineda https://orcid.org/0000-0002-5362-8614

REFERENCES

Alpers, W. (1985). Theory of radar imaging of internal waves. *Nature*, *314*, 245–247. https://doi.org/10.1038/314245a0

Anger, K., Storch, V., Anger, V., & Capuzzo, J. (1985). Effects of starvation on moult cycle and hepatopancreas of stage I lobster (*Homarus americanus*) larvae. *Helgoländer Wissenschaftliche Meeresuntersuchungen*, *39*, 107–116. https://doi.org/10.1007/BF01997445

Annis, E. R. (2004). *Biology and ecology of larval lobsters (*Homarus americanus*): Implications for population connectivity and larval transport*. The University of Maine.

Annis, E. R. (2005). Temperature effects on the vertical distribution of lobster postlarvae (*Homarus americanus*). *Limnology and Oceanography*, *50*, 1972–1982. https://doi.org/10.4319/lo.2005.50.6.1972

Auerswald, L., Freier, U., Lopata, A., & Meyer, B. (2008). Physiological and morphological colour change in Antarctic krill, Euphausia superba: A field study in the Lazarev Sea. *The Journal of Experimental Biology*, *211*, 3850–3858. https://doi.org/10.1242/jeb.024232

Barnes, H. (1956). *Balanus balanoides* (L.) in the firth of Clyde: The development and annual variation of the larval population, and the causative factors. *The Journal of Animal Ecology*, *25*, 72–84. https://doi.org/10.2307/1851

Bartley, D. M., Carlberg, J. M., van Olst, J. C., & Ford, R. F. (1979). Effects of temperature and feeding level on growth of the American lobster, *Homarus americanus*, p. 17. International Council for the Exploration of the Seas Mariculture Committee report. C.M.1979/F:27.

Campbell, A., & Robinson, D. (1983). Reproductive potential of three American lobster (*Homarus americanus*) stocks in the Canadian Maritimes. *Canadian Journal of Fisheries and Aquatic Sciences*, *40*, 1958–1967. https://doi.org/10.1139/f83-225

Castro, J. J., Santiago, J. A., & Santana-Ortega, A. T. (2002). A general theory on fish aggregation to floating objects: An alternative to the meeting point hypothesis. *Reviews in Fish Biology and Fisheries*, *11*, 255–277.

Charmantier, G., Charmantier-Daures, M., & Aiken, D. (1984). Neuroendocrine control of hydromineral regulation in the American lobster *Homarus americanus* H. Milne-Edwards, 1837 (Crustacea, Decapoda): 2. Larval and postlarval stages. *General and Comparative Endocrinology*, *54*, 20–34. https://doi.org/10.1016/0016-6480(84)90194-1

Clancy, M., & Epifanio, C. E. (1989). Distribution of crab larvae in relation to tidal fronts in Delaware Bay, USA. *Marine Ecology Progress Series*, *57*, 77–82. https://doi.org/10.3354/meps057077

Cobb, J., Gulbransen, T., Phillips, B., Wang, D., & Syslo, M. (1983). Behavior and distribution of larval and early jevenile *Homarus americanus*. *Canadian Journal of Fisheries and Aquatic Sciences*, *40*, 2184–2188. https://doi.org/10.1139/f83-252

DiBacco, C., Fuchs, H., Pineda, J., & Helfrich, K. (2011). Swimming behavior and velocities of barnacle cyprids in a downwelling flume. *Marine Ecology Progress Series*, *433*, 131–148. https://doi.org/10.3354/meps09186

Ennis, G. (1975). Behavioral responses to changes in hydrostatic pressure and light during larval development of the lobster *Homarus americanus*. *Journal of the Fisheries Board of Canada*, *32*, 271–281. https://doi.org/10.1139/f75-025

Ennis, G. (1995). Larval and postlarval ecology. In J. R. Factor (Ed.), *Biology of the lobster*, Homarus americanus (pp. 23–46). Academic Press. https://doi.org/10.1016/B978-012247570-2/50025-6

Epifanio, C. E. (1987). The role of tidal fronts in maintaining patches of brachyuran zoaea in estuarine waters. *Journal of Crustacean Biology*, *7*, 513–517. https://doi.org/10.2307/1548299

Factor, J. R. (1995). Introduction, anatomy, and life history. In J. R. Factor (Ed.), *Biology of the lobster*, Homarus americanus (pp. 1–11). Academic Press. https://doi.org/10.1016/B978-012247570-2/50023-2

Fingerman, M. (1985). The physiology and pharmacology of crustacean chromatophores. *American Zoologist*, *25*, 233–252. https://doi.org/10.1093/icb/25.1.233

Fogarty, M. J. (1983). Distribution and relative abundance of american lobster, *Homarus americanus*, larvae: A review. In M. J. Fogarty (Ed.), *NOAA technical report NMFS SSRF-775* (pp. 3–8). National Marine Fisheries Service, NOAA, U.S. Dept. of Commerce.

Fogarty, M. J. (1998). Implications of migration and larval interchange in American lobster (*Homarus americanus*) stocks: Spatial structure and resilience. *Canadian Special Publication of Fisheries and Aquatic Sciences*, 273–284.

Fogarty, M. J., & Idoine, J. S. (1986). Recruitment dynamics in an American lobster (*Homarus americanus*) population. *Canadian Journal of Fisheries and Aquatic Sciences*, *43*, 2368–2376. https://doi.org/10.1139/f86-289

Gendron, L., Lefaivre, D., & Sainte-Marie, B. (2018). Local egg production and larval losses to advection contribute to interannual and long-term variability of American lobster (*Homarus americanus*) settlement intensity. *Canadian Journal of Fisheries and Aquatic Sciences*, 1–14.

Gouveia, G. R., Lopes, T. M., Neves, C. A., Nery, L. E. M., & Trindade, G. S. (2004). Ultraviolet radiation induces dose-dependent pigment dispersion in crustacean chromatophores. *Pigment Cell Research*, *17*, 545–548. https://doi.org/10.1111/j.1600-0749.2004.00191.x

Govoni, J. J., & Grimes, C. B. (1992). The surface accumulation of larval fishes by hydrodynamic convergence within the Mississippi River plume front. *Continental Shelf Research*, *12*, 1265–1276. https://doi.org/10.1016/0278-4343(92)90063-P

Grabe, S. A., Shipman, J. W., & Bosworth, W. S. (1983). Distribution and relative abundance of American lobster, *Homarus* americanus, larvae: A review. In M. J. Fogarty (Ed.), *NOAA technical report NMFS SSRF-775* (pp. 53–57). National Marine Fisheries Service, NOAA, U.S. Dept. of Commerce.

Greenstein, D. M., Alexander, L. C., & Richter, D. E. (1983). Abundance and distribution of lobster larvae (*Homarus americanus*) for selected locations in Penobscot Bay, Maine. In M. J. Fogarty (Ed.), *NOAA technical report NMFS SSRF-775* (pp. 58–61). National Marine Fisheries Service, NOAA, U.S. Dept. of Commerce.

Hamner, W. M. (1988). The "lost year" of the sea turtle. *Trends in Ecology and Evolution*, *3*, 116–118. https://doi.org/10.1016/0169-5347(88)90120-6

Harding, G. C., Pringle, J. D., Vass, W. P., Pearre, S. Jr., & Smith, S. J. (1987). Vertical distribution and daily movements of larval lobsters *Homarus americanus* over Browns Bank, Nova Scotia. *Marine Ecology Progress Series*, *41*, 29–41. https://doi.org/10.3354/meps041029

Harding, G. C., Vass, W. P., & Drinkwter, K. F. (1982). Aspects of larval American lobster (*Homarus americanus*) ecology in St. Georges Bay, Nova Scotia. *Canadian Journal of Fisheries and Aquatic Sciences*, *39*, 1117–1129. https://doi.org/10.1139/f82-149

Harrington, A. M., Tudor, M. S., Reese, H. R., Bouchard, D. A., & Hamlin, H. J. (2019). Effects of temperature on larval American lobster (*Homarus americanus*): Is there a trade-off between growth rate and developmental stability? *Ecological Indicators*, *96*, 404–411. https://doi.org/10.1016/j.ecolind.2018.09.022

Hastings, A., & Botsford, L. W. (2006). Persistence of spatial populations depends on returning home. *Proceedings. National Academy of Sciences. United States of America*, *103*, 6067–6072. https://doi.org/10.1073/pnas.0506651103

Hultgren, K. M., & Mittelstaedt, H. (2015). Color change in a marine isopod is adaptive in reducing predation. *Current Zoology*, *61*, 739–748. https://doi.org/10.1093/czoolo/61.4.739

Incze, L. S., Aas, P., Ainaire, T., & Bowen, M. (2000). Neustonic postlarval American lobsters, *Homarus americanus*, in the western Gulf of Maine: Spatial and interannual variations. *Canadian Journal of Fisheries and Aquatic Sciences*, *57*, 755–765. https://doi.org/10.1139/f00-005

Incze, L. S., & Naimie, C. E. (2000). Modelling the transport of lobster (*Homarus americanus*) larvae and postlarvae in the Gulf of Maine. *Fisheries Oceanography*, *9*, 99–113. https://doi.org/10.1046/j.1365-2419.2000.00125.x

Incze, L. S., & Wahle, R. A. (1991). Recruitment from pelagic to early benthic phase in lobsters *Homarus americanus*. *Marine Ecology Progress Series*, *79*, 77–87. https://doi.org/10.3354/meps079077

Incze, L. S., Wahle, R., Wolff, N., Wilson, C., Steneck, R., Annis, E., Lawton, P., Xue, H., & Chen, Y. (2006). Early life history and a modeling framework for lobster (*Homarus americanus*) populations in the Gulf of Maine. *Journal of Crustacean Biology*, *26*, 555–564. https://doi.org/10.1651/S-2764.1

Incze, L., Xue, H., Wolff, N., Xu, D., Wilson, C., Steneck, R., Wahle, R., Lawton, P., Pettigrew, N., & Chen, Y. (2010). Connectivity of lobster (*Homarus americanus*) populations in the coastal Gulf of Maine: Part II. Coupled biophysical dynamics. *Fisheries Oceanography*, *19*, 1–20. https://doi.org/10.1111/j.1365-2419.2009.00522.x

Juinio, M. A. R., & Cobb, J. S. (1992). Natural diet and feeding habits of the postlarval lobster *Homarus americanus*. *Marine Ecology Progress Series*, *85*, 83–91. https://doi.org/10.3354/meps085083

Kassambara, A. 2023. ggpubr: 'ggplot2' based publication ready plots. R package version 0.6.0.

Kingsford, M. J. (1993). Biotic and abiotic structure in the pelagic environment: Importance to small fishes. *Bulletin of Marine Science*, *53*, 393–415.

Kukulka, T., Plueddemann, A. J., Trowbridge, J. H., & Sullivan, P. P. (2009). Significance of Langmuir circulation in upper ocean mixing: Comparison of observations and simulations. *Geophysical Research Letters*, *36*, L10603. https://doi.org/10.1029/2009GL037620

le Fèvre, J. (1986). Aspects of the biology of frontal systems. *Advances in Marine Biology*, *23*, 163–299. https://doi.org/10.1016/S0065-2881(08)60109-1

Lima-Mendez, G., Faust, K., Henry, N., Decelle, J., Colin, S., Carcillo, F., Chaffron, S., Ignacio-Espinosa, J. C., Roux, S., & Vincent, F. (2015). Determinants of community structure in the global plankton interactome. *Science*, *348*, 1262073. https://doi.org/10.1126/science.1262073

Manly, B. (1997). *Randomization, bootstrap and Monte Carlo methods in biology* (2nd ed.). London: CRC Press.

Metaxas, A. (2001). Behaviour in flow: Perspectives on the distribution and dispersion of meroplanktonic larvae in the water column. *Canadian Journal of Fisheries and Aquatic Sciences*, *58*, 86–98. https://doi.org/10.1139/f00-159

O'Donnell, J. (1990). The formation and fate of a river plume: A numerical model. *Journal of Physical Oceanography*, *20*, 551–569. https://doi.org/10.1175/1520-0485(1990)020<0551:TFAFOA>2.0.CO;2

O'Donnell, J., Marmorino, G. O., & Trump, C. L. (1998). Convergence and downwelling at a river plume front. *Journal of Physical Oceanography*, *28*, 1481–1495. https://doi.org/10.1175/1520-0485(1998)028<1481:CADAAR>2.0.CO;2

Ohman, M. D., & Hirche, H. J. (2001). Density-dependent mortality in an oceanic copepod population. *Nature*, *412*, 638–641. https://doi.org/10.1038/35088068

Pennington, J. T., Rumrill, S. S., & Chia, F.-S. (1986). Stage-specific predation upon embryos and larvae of the Pacific sand dollar, *Dendraster excentricus*, by 11 species of common zooplanktonic predators. *Bulletin of Marine Science*, *39*, 234–240.

Pineda, J. (1999). Circulation and larval distribution in internal tidal bore warm fronts. *Limnology and Oceanography*, *44*, 1400–1414. https://doi.org/10.4319/lo.1999.44.6.1400

Pineda, J., & Reyns, N. (2018). Larval transport in the coastal zone: biological and physical processes. In T. J. Carrier, A. M. Reitzel, & A. Heyland (Eds.), *Evolutionary ecology of marine invertebrate larvae* (pp. 141–159). Oxford University Press.

Pineda, J., Reyns, N., & Starczak, V. R. (2009). Complexity and simplification in understanding recruitment in benthic populations. *Population Ecology*, *51*, 17–32. https://doi.org/10.1007/s10144-008-0118-0

Pineda, J., Rouse, S., Starczak, V., Helfrich, K., & Wiley, D. (2020). Response of small sharks to nonlinear internal waves. *Limnology and Oceanography*, *65*, 707–716. https://doi.org/10.1002/lno.11341

Platt, T., Fuentes-Yaco, C., & Frank, K. T. (2003). Spring algal bloom and larval fish survival. *Nature*, *423*, 398–399. https://doi.org/10.1038/423398b

Quinn, B. K. (2017). Threshold temperatures for performance and survival of American lobster larvae: A review of current knowledge and implications to modeling impacts of climate change. *Fisheries Research*, *186*, 383–396. https://doi.org/10.1016/j.fishres.2016.09.022

Rumrill, S. S. (1990). Natural mortality of marine invertebrate larvae. *Ophelia*, *32*, 163–198. https://doi.org/10.1080/00785236.1990.10422030

Schneider, C. A., Rasband, W. S., & Eliceiri, K. W. (2012). NIH image to ImageJ: 25 years of image analysis. *Nature Methods*, *9*, 671–675. https://doi.org/10.1038/nmeth.2089

Shanks, A. L. (1985). Behavioral basis of internal-wave induced shoreward transport of megalopae of the crab *Pachygrapsus crassipes*. *Marine Ecology Progress Series*, *24*, 289–295. https://doi.org/10.3354/meps024289

Shanks, A. L., Largier, L., Brink, L., Brubaker, J., & Hooff, R. (2000). Demonstration of the onshore transport of larval invertebrates by the shoreward movement of an upwelling front. *Limnology and Oceanography*, *45*, 230–236. https://doi.org/10.4319/lo.2000.45.1.0230

da Silva, J. C. B., Ermakov, S. A., Robinson, I. S., Jeans, D. R. G., & Kijashko, S. V. (1998). Role of surface films in ERS SAR signatures of internal waves on the shelf. 1. Short-period internal waves. *Journal of Geophysical Research*, *103*, 8009–8031. https://doi.org/10.1029/97JC02725

Smith, M. R. (2017). *Ternary: An R package for creating ternary plots*. Comprehensive R Archive Network.

Smith, K. N., & Herrkind, W. F. (1992). Predation on early juvenile spiny lobsters *Panulirus argus* (Latreille): Influence of size and shelter. *Journal of Experimental Marine Biology and Ecology*, *157*, 3–18. https://doi.org/10.1016/0022-0981(92)90070-Q

Stevens, M. (2016). Color change, phenotypic plasticity, and camouflage. *Frontiers in Ecology and Evolution*, *4*, 51.

Templeman, W. (1936). The influence of temperature, salinity, light and food conditions on the survival and growth of the larvae of the lobster (*Homarus americanus*). *Journal of the Biological Board of Canada*, *2*, 485–497. https://doi.org/10.1139/f36-029

Umbers, K. D., Fabricant, S. A., Gawryszewski, F. M., Seago, A. E., & Herberstein, M. E. (2014). Reversible colour change in Arthropoda. *Biological Reviews*, *89*, 820–848. https://doi.org/10.1111/brv.12079

Verity, P. G., & Smetacek, V. (1996). Organism life cycles, predation, and the structure of marine pelagic ecosystems. *Marine Ecology Progress Series*, *130*, 277–293. https://doi.org/10.3354/meps130277

Wahle, R. A., & Steneck, R. S. (1991). Recruitment habitats and nursery grounds of the American lobster *Homarus americanus*: A demographic bottleneck? *Marine Ecology Progress Series*, 231–243.

Warren, J. D., Stanton, T. K., Wiebe, P. H., & Seim, H. E. (2003). Inference of biological and physical parameters in an internal wave using multiple-frequency, acoustic-scattering data. *ICES Journal of Marine Science*, *60*, 1033–1046. https://doi.org/10.1016/S1054-3139(03)00121-8

Whitney, J. L., Gove, J. M., McManus, M. A., Smith, K. A., Lecky, J., Neubauer, P., Phipps, J. E., Contreras, E. A., Kobayashi, D. R., & Asner, G. P. (2021). Surface slicks are pelagic nurseries for diverse ocean fauna. *Scientific Reports*, *11*, 3197. https://doi.org/10.1038/s41598-021-81407-0

Zeldis, J. R., & Jillet, J. B. (1982). Aggregation of pelagic *Munida gregaria* (Fabricius) (Decapoda, Anomura) by coastal fronts and internal waves. *Journal of Plankton Research*, *4*, 839–857. https://doi.org/10.1093/plankt/4.4.839

How to cite this article: Pineda, J., Tepolt, C., Starczak, V., Alatalo, P., & Shapiro, S. (2023). Concentration and condition of American lobster postlarvae in small-scale convergences. *Fisheries Oceanography*, 1–17. https://doi.org/10.1111/fog.12657